Absorption of Electromagnetic Radiation in an Advanced Propulsion System

Anil Gulati* and Charles L. Merkle†
The Pennsylvania State University, University Park, Pennsylvania

The concept of beamed energy propulsion is studied in detail with emphasis on the strong interaction between a laser beam and a flowing gas. The problem is modeled in a one-dimensional sense using a "pseudo-convergent" optical beam. The beam convergence enables the mass flow to be dictated by the nozzle throat rather than by the eigensolution for the laser supported plasma. The results show that the mass flux and thrust achieved through a fixed nozzle is nearly independent of the incoming intensity, a result which is in sharp contrast to calculations based on laser supported plasma eigenvalues. The range of laser intensities which can be used with a given nozzle is also limited, but the results indicate that the location of the plasma inside the absorber can be controlled by the nozzle and incident beam. The effect of laser wavelength on the laser supported plasma wave is also shown and the effects of frozen flow on the propulsive performance are estimated.

Nomenclature

A = cross sectional area of chamber
A_L = cross sectional area of beam
e = total energy per unit volume
F = flux vector
h^0 = stagnation enthalpy
I = local intensity
I_0 = incoming intensity of beam
I_1, I_2 = integrals defined in Eqs. (13) and (14)
I_{sp} = specific impulse
k = absorptivity of gas, m^{-1}
$\dot{m}$ = mass flow
p = pressure
P = power (local) of beam
P_0 = initial power of beam
q_L = radial loss of energy
q_r = energy transported in axial direction
q_s = rate of energy absorption
S = source vector
T = temperature
T_∞ = temperature at infinity
T_0 = temperature at $x=0$
u = velocity
U = vector of conserved variables
x = axial distance
ϵ = internal energy
λ, μ = viscosity coefficients
λ_c = thermal conductivity
λ_R = radiative conductivity
ρ = density
σ = stress

Introduction

BEAMED energy propulsion promises to provide high specific impulse and high thrust density. The concept is based upon transmitting energy from a remote site to a spacecraft by means of a high-intensity beam of electromagnetic energy. After being received at the propulsive vehicle, the energy is converted into random kinetic energy of a working fluid. The fluid is then expanded through a conventional nozzle to produce thrust. Although the energy can be transferred to the flux by an indirect path (such as by using it to heat a metal surface which is subsequently cooled by the fluid), the present paper will consider only the direct path wherein the electromagnetic energy is directly absorbed by the fluid. The beamed energy sources considered will be restricted to lasers radiating in the infrared region.

The absorption characteristics of any gas are very complex and the dynamics of the strong interaction between an intense radiation field and a flowing gas are largely unknown. Hydrogen has been chosen as a working fluid for the present study primarily because of its low molecular weight and its capability for absorbing in the frequency range of interest. Like most gases, hydrogen is poor absorber at low temperatures, but at elevated temperatures (around 10,000 K) where ionization begins, its absorptivity increases dramatically. When free electrons are present, the inverse bremsstrahlung absorption mechanism, which is a continuum absorption mechanism, reduces the photon mean free path to very short distances. The incoming gas in a propulsive system is, however, cold and some mechanism must exist to heat the gas to these elevated temperatures at which inverse bremsstrahlung absorption can take place. This preheating of the incoming cold gas represents an important part of the dynamics of the radiation/gas dynamic interaction. The additional parts of this interaction include the losses from the plasma and the flow through a propulsive nozzle. The present paper is directed toward a better understanding of this interaction and toward predicting the performance of a laser propulsion system. To focus attention on the fundamental characteristics of this interaction, it will be treated in a one-dimensional manner.

Physics of the Problem

The concept of laser propulsion is illustrated schematically in Fig. 1. The high-intensity beam enters through a window in the upstream end of the absorption chamber, which replaces the combustor in a conventional chemical propulsion engine. Most of the energy is absorbed near the foucs of the beam in a hot plasma region which converts the radiant energy into internal energy of the fluid. The presence of the plasma, which is denoted as a laser supported plasma (LSP), gives rise to the mechanisms which preheat the fresh incoming gases to temperatures at which inverse bremsstrahlung can take place.

Presented as Paper 82-1950 at the AIAA/JSASS/DGLR 16th International Electric Propulsion Conference, New Orleans, La., Nov. 17-19, 1982; submitted Dec. 27, 1982; revision received July 5, 1983.

*Graduate Assistant, Mechanical Engineering.
†Professor, Mechanical Engineering. Member AIAA.

The mechanisms include heat feedback by thermal conduction and radiation, and in addition, may also include the feedback of a nonequilibrium concentration of free electrons to the cooler gas upstream of the plasma. Although the presence of excess electrons could have a dramatic effect on the absorption characteristcs of the cooler gas, and may be important in the propagation of the plasma, only equilibrium effects have been included in the present results. The combined effects of these multiple mechanisms is to yield a unique propagation speed of the plasma which depends on the local intensity of the beam, the pressure, and the optical configuration. The plasma can be held stationary in the absorption chamber by maintaining the gas flow precisely equal to the propagation speed of the plasma. This precise gas flow rate constitutes an eigenvalue solution to the problem.

The flow velocities required to hold the plasma stationary are relatively low and, hence, the pressure is nearly constant throughout the absorption region. The plasma wave constitutes a thin region of steep temperature rise followed by a gradual decay of temperature due to the domination of radiative losses over the absorption of the incoming beam which has been almost completely absorbed by then.

Raizer[1] was one of the first researchers to study the propagation characteristics of a laser supported plasma. By replacing the momentum equation by a statement that the pressure was a constant (as alluded to above) he obtained an ordinary differential equation for the temperature profile through the plasma. The mass flow through the plasma then emerges as an eigenvalue solution to this ordinary differential equation. Similar analyses along this line have also been reported.[2,3] Kemp and co-workers have expanded this basic scheme by including temperature-dependent thermodynamic properties of the gas. They reported calculations for the eigenvalue mass flow rate in hydrogen for several conditions. In addition, they modeled the effects of radiation losses in the radial direction to take into account this important nonadiabatic character of the problem.[4-6]

Experimental realizations of the laser supported plasma also have been reported. Most of the earlier results were for plasmas in air,[1,7] but the establishment of a plasma in hydrogen has also been reported recently.[8,9]

The present research extends the previous analytical work, which applied only to flows in constant area ducts, to the flow characteristics of an absorber/nozzle combination. The unique character of the absorber/nozzle combination is that two unrelated mechanisms strive to define the mass flow rate. The laser supported plasma admits only one mass flow for a given intensity, whereas the choked throat also admits a single flow for given upstream conditions. The operation of the absorber/nozzle combination requires that these two mass flows be identically the same. It appears that the only path around this dilemma is to switch from a collimated to a convergent beam. (Indeed, a convergent beam is also needed to ensure static stability of the plasma in a constant area duct.[4]) This is the approach followed in the present analysis; the incoming beam is assumed to be focused.The choked throat of the nozzle is thus free to set the mass flow while the plasma moves axially along the varying intensity beam until it reaches a local intensity at which the eigenvalue solution just matches the choking conditions at the throat. The presence of the nozzle throat, however, greatly restricts the range of intensities which can be used, as is discussed later. The problem is thus reduced from a simple eigenvalue problem to an interactive problem in which the geometry and other relevant parameters determine the mass flow rate required to sustain the plasma.

The temperature profile in the plasma, its thickness, and its location depend on other parameters such as the f number of the lens, the wavelength of the laser beam, the incoming laser power, and the geometry of the nozzle. Such functional dependence on various parameters is also a subject of study in the present work.

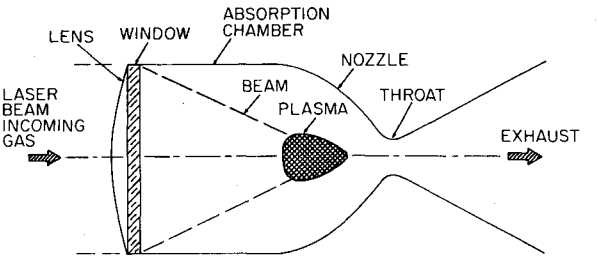

Fig. 1 Schematic illustration of rocket propulsion concept.

Method of Solution

The complete equations of motion which represent the one-dimensional interactions between the incident beam and the flowing gas are given in vectorial form as

$$\partial F/\partial x = S \tag{1}$$

where

$$F = \begin{bmatrix} \rho u A \\ (\rho u^2 + \sigma) A \\ (e+\sigma) uA - \lambda_c A (\mathrm{d}T/\mathrm{d}x) + q_R A \end{bmatrix} \tag{2}$$

$$S = \begin{bmatrix} 0 \\ \sigma \mathrm{d}A/\mathrm{d}x \\ (q_s - q_L) A \end{bmatrix} \tag{3}$$

The stress tensor σ is

$$\sigma = p(\lambda + 2\mu)\,\mathrm{d}u/\mathrm{d}x \tag{4}$$

and the total energy e is

$$e = (\epsilon + u^2/2)\rho \tag{5}$$

These three equations represent the continuity, momentum, and energy equations, respectively. The first two are in their standard form, but the third equation contains several new terms which need further elaboration. These new terms describe the effects of the incident beam on the energy balance in the flow. The main constituents of this balance are the convection and thermal conduction of energy, the energy transport by radiation, the loss of energy to the surroundings, and the absorption of laser energy.

The rate of energy absoprtion q_s is computed from the local intensity of the beam and the gas absorptivity as

$$q_s = kI \tag{6}$$

where it is assumed that the beam is absorbed uniformly across the entire flow area. The local intensity I is, in turn, determined from the amount of power remaining in the beam divided by the area of the beam A_L.

$$I = \frac{P}{A_L} = \frac{P_0 - \int_0^x kIA\,\mathrm{d}x}{A_L} \tag{7}$$

where P_0 represents the initial power in the beam. It is this definition of the beam area which is used to simulate the effect of a convergent beam.

The term q_L represents the radial loss of energy from the hot flowing gas to the surroundings. Such heat losses in the direction perpendicular to the flow cannot be computed from the first principles in a one-dimensional analysis, so we have

chosen to model this loss in the phenomenological sense suggested by Kemp and Root.[5] Their model for the radiative losses depends upon the temperature and the radius of the plasma core. The intent of this loss term is to include such effects in a qualitative sense while retaining the simplicity of the one-dimensional formulation.

The energy transported in the axial direction by radiation has also been modeled in a simplified manner and is represented by the term q_R in Eq. (2). This radiation is not lost from the flow, but instead serves as a propagation mechanism for the plasma. For radiation to be an effective transport mechanism it must be strongly absorbed by the incoming cool gas (which is simultaneously almost transparent to the laser radiation). In addition, the radiation emitted from the interior of the plasma must not be absorbed within the plasma. The only portion of the radiation that satisfies these two criteria is that involving transitions to the ground state. Assuming that the temperature of the gas in the plasma does not change appreciably over a photon mean free path, the radiation transport is approximated by the radiation conduction approximation

$$\frac{dq_R A}{dx} = -\frac{d}{dx}\left(\lambda_R A \frac{dT}{dx}\right) \tag{8}$$

The conduction approximation is justified here since the radiation from the plasma core is absorbed in a very thin region ahead of the core. The terms defined in Eqs. (6-8) complete the definition of the energy equation as given in Eqs. (1) and (2).

Although in principle Eq. (1) can be solved to obtain the flowfield throughout the entire nozzle, numerous factors make this task difficult. To circumvent these problems in the present analysis we choose to make one further simplification. This simplification is obtained by dividing the flow domain into two regions: the constant area absorption chamber where the velocities are low and the absorption rates are high, and the nozzle where the absorption rates are low but the velocities are high. By choosing a sufficient absorber length, the complex interaction between the radiation and the gas dynamics is made to take place within the constant area section. Simultaneously, most of the acceleration is made to occur inside the nozzle.

The presence of low velocities within the absorber allows the equations governing the flow in this region to be simplified in the same manner as was used by the earlier researchers.[1-6] In particular, the momentum equation is replaced by the statement that the pressure is a constant. The remaining two equations can then be combined into a single second-order differential equation

$$\frac{d}{dx}\dot{m}h^0 - \frac{d}{dx}A(\lambda_c+\lambda_R)\frac{dT}{dx} = kIA - q_L A \tag{9}$$

The equations for the nozzle are solved by means of an implicit numerical technique[10] which is based upon the time-marching solution of the unsteady equations,

$$\frac{\partial U}{\partial t} + \frac{\partial F}{\partial x} = S \tag{10}$$

where U is the unknown vector

$$U = (\rho A, \rho u A, eA)^T \tag{11}$$

and T denotes transpose. The vectors F and S remain unchanged, except that the laser absorption term is dropped. The solutions of these two portions of the flow and the coupling between them is described in the following subsections.

Absorption Chamber

The flow in the absorption chamber is governed by the single differential equation given above, Eq. (9). This equation can be integrated twice to obtain an integral expression for the temperature. Applying the boundary conditions that the temperature gradient vanishes far upstream where the flow stats from a known temperature, T_∞, and neglecting absorption up to the location $x=0$ where $T=T_0$ gives

$$T = \int_0^x \frac{\dot{m}(h^0 - h^0_\infty)}{A(\lambda_c+\lambda_R)}\,dx - \int_0^x \frac{I_1+I_2}{A(\lambda_c+\lambda_R)}\,dx + T_0 \tag{12}$$

where the integals I_1 and I_2 are given by

$$I_1 = \int_0^x kIA\,dx \tag{13}$$

and

$$I_2 = -\int_0^x q_L\,dx \tag{14}$$

This equation is solved numerically by an iterative process similar to that used previously,[5] to determine the unique mass flow which satisfies the equation for each particular intensity level and ℓ number configuration. Care was taken to select a starting temperature T_0 which did not affect the final results. Typically, a value of 10,000 K was chosen. In addition, the rapid variation of the shape of the temperature profile in the plasma required a careful, solution-dependent control of the grid spacing.

Nozzle

The governing equations for the nozzle were solved using MacCormack's time-dependent implicit scheme[10] to obtain steady-state solutions for various values of inlet stagnation temperature and nozzle area ratios. At the nozzle entrance, the stagnation pressure and temperature were specified as boundary conditions. The nozzle was maintained choked throughout and so at the downstream boundary the flow was always supersonic. Consequently, downstream boundary conditions were obtained by extrapolation from inside the domain. The temperature profile and required mass flux were obtained parametrically for various values of the nozzle area ratio and stagnation temperture.

Matching Between the Eigenvalue and the Nozzle Mass Flux

The flowfields in the absorption chamber and nozzle were solved separately and matched to obtain a solution for the entire flowfield. For the absorption chamber a series of mass fluxes corresponding to eigenvalue solutions were determined, along with the corresponding exit stagnation temperatures, using the incoming laser intensity as a parameter. Similarly, for the nozzle a series of curves of mass flux vs inlet tem-

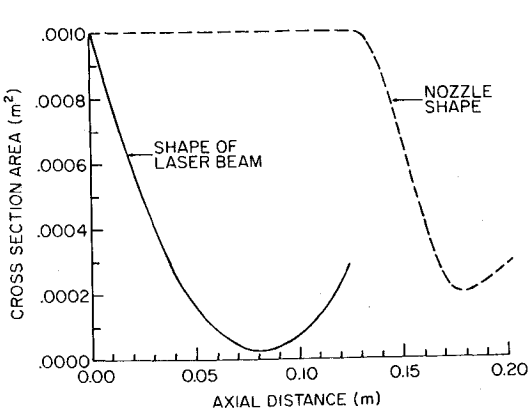

Fig. 2 Geometry of absorber/nozzle combination showing outline of laser beam convergence and nozzle shape.

perature were determined using the nozzle area ratio as a parameter. The two sets of two curves thus generated cover the whole solution domain and any point of intersection of these curves represents a matched solution of the mass flow corresponding to both the intensity and the nozzle geometry of interest.

Discussion of Results

The basic geometry of the absorber/nozzle combination which was used for the calculations is shown in Fig. 2. The absorber was a constant area section 120 mm long. This was followed by the nozzle whose shape was described by a cubic polynomial. The coefficients of the polynomial were determined by specifying the axial length of the convergent section of the nozzle and the throat height and by requiring the wall slope to vanish at the throat and to be continuous at the absorber/nozzle juncture. For all cases, the length of the nozzle was chosen to be 60 mm. A series of different nozzle throat sizes with this basic shape were considered. The particular throat size is classified by its "area ratio" which describes the ratio of the throat to the absorber area. This is not to be confused with the more common definition of the nozzle area ratio which describes the divergence of the supersonic side of the nozzle.

Since conditions in the supersonic portion of the nozzle do not affect conditions upstream of the throat, this part of the geometry is not defined in Fig. 2. For the thrust and specific impulse claculations, an infinite expansion ratio was assumed (although some calculations are also presented for a convergent nozzle), so that precise definitions of the supersonic portion of the nozzle were not required.

Also shown in Fig. 2 is an outline of the convergence pattern of the incoming laser beam. Consistent with the one-dimensional approximation, the size of the beam was assumed to decrease to a "focal" point after which it again increased. The convergence ratio used was 100:1 in area (10:1 in diameter). The absorption of the beam in the presence of this varying intensity pattern was computed by keeping track of the fraction of incoming power which had been absorbed.

One of the most notable characteristics of a laser supported plasma arises because of the extremely rapid variation of the absorption coefficient of a gas as a function of temperature. The variations which were used for the present calculations are shown on Fig. 3. The absorption coefficient is given for each of three wavelengths: 2.2, 10.6, and 106 μm. The 2.2 μm wavelength was chosen because it is a wavelength at which a laser beam can be propagated through the atmosphere with minimum losses[11]; the 10.6 μm wavelength corresponds to a CO_2 laser beam; while the 106 μm wavelength was selected arbitrarily to give a wider variation in wavelength so as to obtain a better undertstanding of the effects of wavelength on the behavior of the laser supported plasma. The temperature dependence of the absorption coefficients shown in Fig. 3 have been calculated from existing models for hydrogen.[6]

The results in Fig. 3 show that the absorption coefficient increases rapidly with wavelength. This suggests that the 106 μm wavelength is best suited for absorption, but results indicate that complete absorption can be obtained within a few centimeters at all three wavelengths. The different levels of absorption coefficient do, however, have a dramatic effect on the temperature distribution inside the plasma as shown in Fig. 4. The calculations on this figure are for the incoming intensity, 5×10^8 W/m^2, and the same ℓ number, 2.5. For the same incident power, the axial extent of the absorbing region decreases as does the peak temperature when the laser wavelength is increased. This is a result of the increase in mass

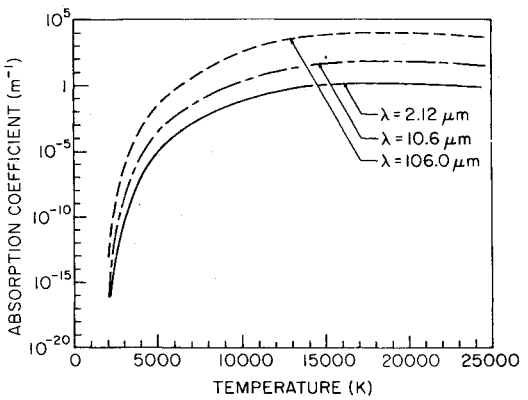

Fig. 3 Absorption coefficient as a function of temperature for hydrogen for three wavelengths; pressure, 1 atm.

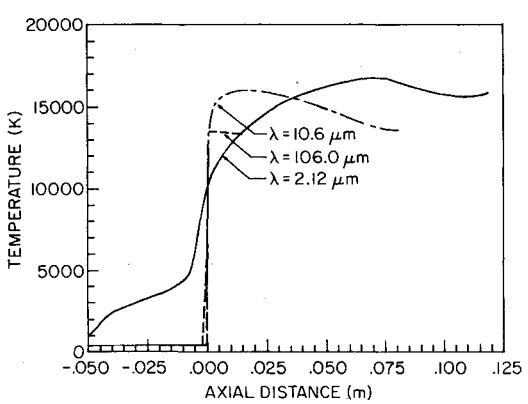

Fig. 4 Eigenvalue solutions of the temperature profile as a function of wavelength for an incoming laser intensity of 5×10^8 W/m^2 and the same optics.

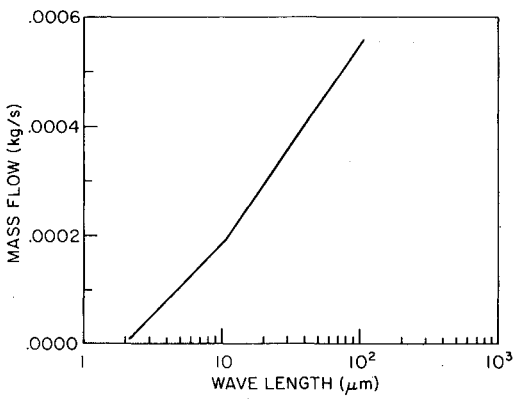

Fig. 5 Mass flow rate as a function of wavelength for the temperature profiles shown in Fig. 4.

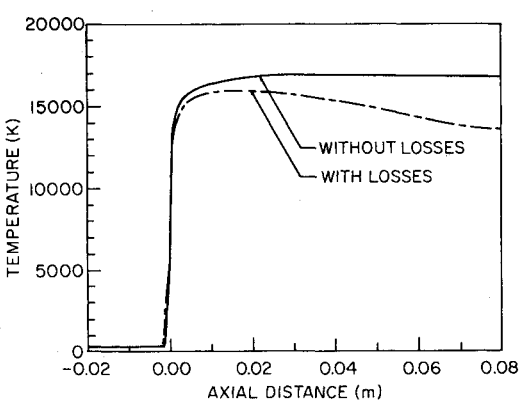

Fig. 6 Effect of heat loss on eigenvalue solution. Incoming laser intensity 5.0×10^8 W/m^2; wavelength, 10.6 μm.

flow with wavelength as is shown in Fig. 5. The most dramatic effect of changes in the wavelength appear to be their effect on the power level required to sustain the plasma. Calculations showed that a plasma could be sustained to intensities as low as 100 W/m^2 for the 106 μm case, but substantially higher powers were required at the other wavelengths. (The intensity required to sustain a plasma continues to decrease with wavelength beyond 106 μm, and is considerably lower in the microwave range. Problems with long-range transmission, however, as well as lack of control over the plasma volume, make operation at these longer wavelengths unlikely. Also, the absorption analysis has to be replaced by the more complete Joule-heating formulation from Maxwell's equations at these longer wavelengths.) Referring again to the lower-temperature portion of the curves in Fig. 4, we note that the kinks in this region are a result of the fairly strong temperature variation of the thermal conductivity in this region.

As is evident from Fig. 4, the presence of a radiation loss term in the equation implies that the plasma temperature reaches a peak as the energy is being absorbed, and then, downstream of this peak, the temperature again decreases because of the cooling. An example of the effect of the radiation losses on the overall temperature profile is given in Figs. 6 and 7. Figure 6 compares a temperature profile with no heat loss with a profile which includes the effect of the radiation loss model. Curves of the heat absorbed and heat lost per unit length are given in Fig. 7. The present loss model predicts radiative losses of approximately 60% for this absorber/nozzle combination. Substantial reductions in this loss could be realized by shortening the absorber. Nevertheless, it is noted that this model of the losses is not to be interpeted as being quantitatively realistic, but is only intended to give an indication of the qualitative effects of radiative losses on the behavior of the plasma. Quantitative estimates of these losses require the use of a two-dimensional analysis.

A comparison of the mass flux through a plasma in a constant area duct (the eigenvalue solution) and that through a plasma in a propulsion engine (i.e., with a fixed area, choked throat downstream) is shown on Fig. 8 as a function of the incoming intensity. For the constant area duct calculation, the mass flow through the plasma increases rapidly with increasing intensity; whereas, when the flow rate is controlled by the nozzle throat, the mass flux is a very weak function of temperature and has the opposite slope. It is interesting to note in the case of the duct flow solutions that despite the increased mass flow, the peak temperature in the plasma also increases with intensity. This is seen on Fig. 9 which shows temperature profiles in the plasma for the eigenvalue calculations. These temperature profiles have been extended through a nozzle throat, but a different area has been selected for each calculation to match the eigenvalue solution. In all three cases shown, the power in the laser beam has been absorbed before the flow reaches the entrance to the nozzle, so no heat is deposited in this region. The radiative losses are, however, computed throughout the nozzle; and these losses combine with the acceleration effects to reduce the temperature.

Returning again to Fig. 8, we also note that for the nozzle calculation the range of variation in intensity is severely limited, and that a wider variation can only be obtained by considering different area ratios. The reason for this is that as the intensity is decreased, the plasma moves from the upstream end of the absorber toward the focal point. Thus the incoming intensities are limited to those which place the

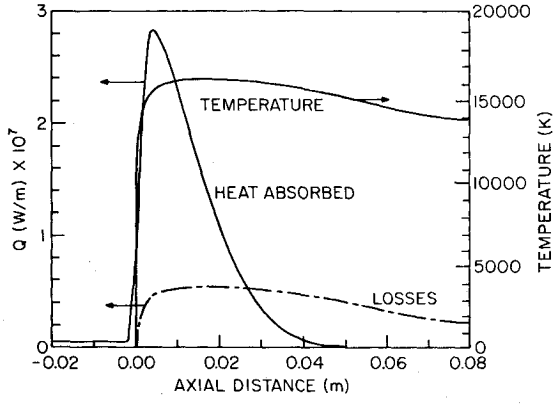

Fig. 7 Temperature profiles showing heat absorbed per unit length and radiation heat loss per unit length. Incoming laser intensity 5.0×10^8 W/m^2; wavelength, 10.6 μm.

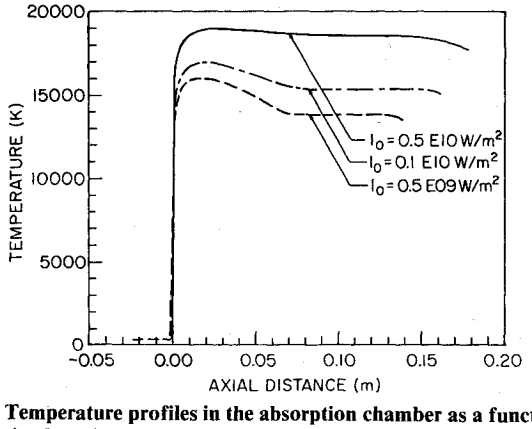

Fig. 9 Temperature profiles in the absorption chamber as a function of incoming laser intensity 10.6 μm; wavelength, 1 atm.

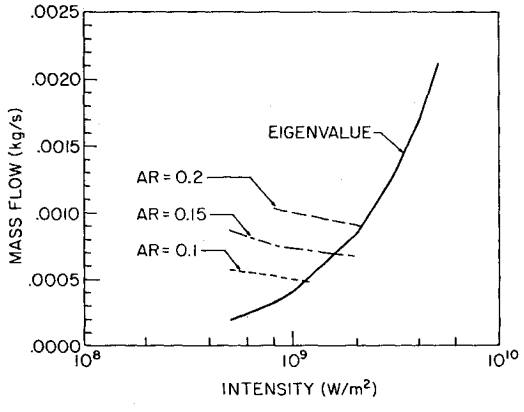

Fig. 8 Mass flow rate as a function of incoming beam intensity for the eigenvalue and the nozzle solution at 10.6 μm. AR denotes area ratio.

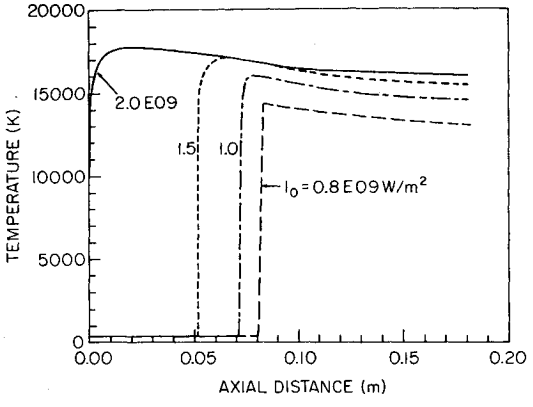

Fig. 10 Temperature profile in the absorption chamber as a function of incoming intensity for a given nozzle geometry. Nozzle area ratio, 0.15; wavelength, 10.6 μm.

plasma between the lens and the focus. This is seen more clearly in Fig. 10 which shows the temperature profiles for the choked throat case. (Note Fig. 10 is identical to Fig. 9 except that Fig 10 shows temperature profiles for a single throat area while Fig. 9 shows temperature profiles for three different throat areas.) Figure 10 clearly shows the role of the choked throat in displacing the profile axially in the nozzle. In practice, the plasma cannot be placed against the window which admits the laser beam into the absorber and it will be necessary to control the plasma location to prevent window damage (in the case of a material window) or propagating the plasma into the window flow (in the case of an aero-window). The results in this figure suggest that this control can be accomplished by a proper choice of the incoming intensity and the nozzle throat area.

The ideal thrust and specific impulse which can be obtained from the laser propulsion system are given on Figs. 11 and 12. These figures show the performance variations as a function of laser intensity for the same two conditions: the eigenvalue solution for the flow in a duct, and the solutions for the flow through a fixed nozzle throat area. The duct solutions again require a different throat area for each incoming intensity. As can be seen from Figs. 11 and 12, the thrust corresponding to the eigensolution increases rapidly with incoming intensity, whereas the specific impulse increases slowly. These performance results are an evidence of the analogous variations in the mass flow rate and peak temperature which were described earlier for the duct flow calculations.

In a realistic application, the performance of a laser thruster would not reach the ideal levels quoted in Figs. 11 and 12. The actual performance would depend upon provisions for wall cooling and losses from the system.

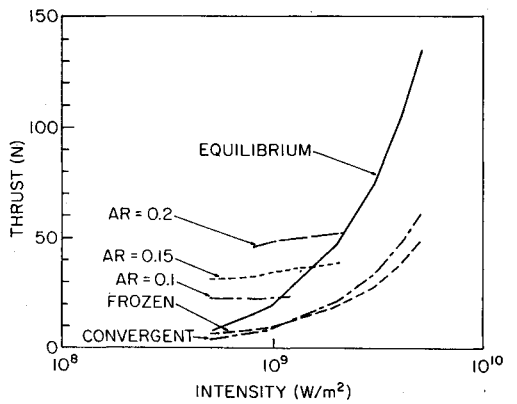

Fig. 11 Thrust as a function of incoming intensity for the eigenvalue solution and for various fixed nozzle geometries, 10.6 μm.

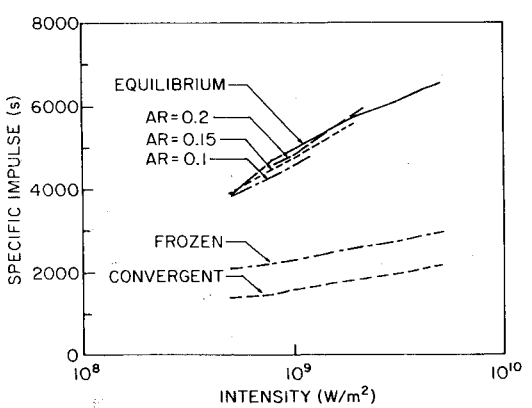

Fig. 12 Specific impulse as a function of incoming intensity for the eigenvalue solution and for various fixed nozzle geometries, 10.6 μm.

Some means of wall protection will certainly be required at these temperature levels. The most attractive concept is the use of a layer of cool buffer gases between the hot central plasma and the walls and a careful control of the plasma volume. The effect of this additional cool gas on performance depends upon the degree of mixing which is achieved, but its presence will lower the specific impulse while increasing the thrust.

The dominant loss mechanism in a laser thruster will most probably be the result of nonequilibrium chemical kinetic effects. In the presence of a finite length divergent section, the highly energetic reattachment and recombination reactions cannot be exprected to remain at equilibrium. The extent by which they are out of equilibrium will depend upon the pressure level and the nozzle length, but at the high flow velocities of the hydrogen atoms and ions, there will be little time to reach equilibrium before the particles are outside the nozzle. An estimate of these nonequilibrium effects based on assuming the kinetics freeze at the nozzle throat is also shown on Figs. 11 and 12. (These simple frozen flow calculations are in qualitative agreement with more complete kinetics calculations of similar conditions reported recently.[12]) As can be seen, the effects of kinetrics can be very important for laser propulsion, although it is noted that the use of a surrounding layer of hydrogen to cool the nozzle may be able to reduce this penalty.[13] As a means of comparison, the performance for a simple convergent nozzle is also shown. If frozen losses are near the maximum indicated, it is seen that the use of a divergent section gives only marginal performance improvement over the convergent nozzle.

The second set of curves on Figs. 11 and 12 are for the fixed throat area conditions. For this case, only the equilibrium conditions are given. Similar effects of frozen flow are to be expected. These fixed nozzle results are analogous to those discussed on Fig. 8. The variation of thrust with intensity is limited because of the aforementioned limits of intensity changes, and because the mass flux through the engine is nearly independent of the intensity. Similar small variations in I_{sp} are also noted.

Summary

The flow processes inside a laser propulsion engine have been reviewed. To simplify the analysis, the problem was treated in a one-dimensional sense and the flowfield was split into two regions. The first region included the absorber and the radiation/gas dynamic interaction. The second region covered the acceleration through the nozzle to supersonic speeds. The flow in the absorber was solved by formulating the equations as an eigenvalue problem in a manner similar to that used by previous researchers. The flow in the nozzle was determined from the complete unsteady equations using an implicit numerical technique.

One characteristic of this problem is that a precise mass through-flow rate is detemined in each of the two regions. In the absorber the mass flux is the eigenvalue and in the nozzle it is the value corresponding to choking. To match these two flows it is necessary to consider a focused beam which will allow the plasma to seek an appropriate axial location at which these two mass flux requirements are satisfied simultaneously. Results based upon this matching scheme showed that although the mass flux determined by the eigenvalue system increases rapidly with laser intensity, the mass flux through the absorber/nozzle combination actually decreases slightly as the intensity is increased. Because the nozzle throat controls the mass flow rate the range of beam intensities which can be used with a given geometry is limited to within a narrow band.

The effect of changes in the laser wavelength was also investigated. The results showed even though the absorption coefficient decreases at the shorter wavelengths, a 2.2 μm beam can be absorbed in a distance of a few centimeters in pure hydrogen. In general, however, these shorter

wavelengths require more intense radiation to support the plasma.

Finally, the thrust and specific impulse which can be obtained from a laser propulsion system has been presented. The specific impulses determined in this manner are unrealistically high because applications will require the addition of a cool layer of gas to protect the walls. Estimates of the effect of this cooling flow on performance, however, require a two-dimensional analysis.

Acknowledgment

This work was sponsored by the Air Force Office of Scientific Research under Contract AFOSR 82-0083.

References

[1]Raizer, Yu. P., *Laser-Induced Discharge Phenomena,* edited by G.C. Vlases and Z.A. Pietrzyk, Consultants Bureau, New York, 1977.

[2]Jackson, J.P. and Nielsen, P.E., "Role of Radiative Transport in the Propagation of Laser Supported Combustion Waves," *AIAA Journal,* Vol. 12, Nov. 1974, p. 1498.

[3]Boni, A.A. and Su, F.Y., "Propagation of Laser Supported Deflagration Waves," *Physics of Fluids,* Vol. 17, Feb. 1974, p. 340.

[4]Kemp, N.H. and Lewis, P.F., "Laser Heated Thruster—Interim Report," NASA CR-161665, Feb. 1980.

[5]Kemp, N.H. and Root, R.G., "Analytical Study of Laser Supported Combustion Waves in Hydrogen," *Journal of Energy,* Vol. 3, Jan. 1979, p. 40.

[6]Kemp, N.H and Krech, R.H., "Laser Heated Thruster—Final Report," NASA CR-161666, Sept. 1980.

[7]Keefer, D.R., Hendrickson, B.B., and Braerman, W.F., "Experimental Study of a Stationary Laser-Sustained Air Plasma," *Journal of Applied Physics,* Vol. 46, March 1975, p. 1080.

[8]Conrad, R.W., Roy, E.L., Pyles, C.E., and Magnum, D.W., "Laser Supported Combustion Wave Ignition in Hydrogen," Redstone Arsenal, Huntsville, Ala., Army Missile Command Tech. Rept. RH-80-1, 1980.

[9]Fowler, M.C. and Smith, D.C., "Propagation of a CW Laser Beam Through a Moving Stagnation Zone," *AIAA Journal,* Vol. 19, Aug. 1981, p. 1019.

[10]MacCormack, R.W., "A Numerical Method for Solving the Equations of Compressible Viscous Flow," AIAA Paper 81-0110, Jan. 1981.

[11]Rather, J.G., "Laser Propulsion Studies," BDM Corporation, McLean, Va., Rept. BDM/W-80-652-TR, 1980.

[12]Jones, L.W. and Keefer, D.R., "NASA's Laser-Propulsion Project," *Astronautics & Aeronautics,* Vol. 20, Sept 1982, p. 66.

[13]Merkle, C.L., "The Potential for Using Laser Radiation to Supply Energy for Propulsion," *Orbit Raising and Maneuvering Propulsion: Research Status and Needs, Progress in Astronautics and Aeronautics Series,* edited by L. Caveny, in press.